# Threat Evasion and Information Propagation in Cognitive Flocks — Supplementary Information —

Priyanka Iyer,[1] Cecilia Soroco,[2] and Gerhard Gompper[1,*]

[1] *Theoretical Physics of Living Matter, Institute for Advanced Simulation, Forschungszentrum Jülich, 52425 Jülich, Germany*

[2] *University of British Columbia, Vancouver, BC V6T 1Z4, Canada*

## S1. CALCULATION APPROACH FOR RANK CURVES

To characterize the propagation of turning information through the flock, we calculate the rank curve $r(t)$, representing the order in which each agent initiates turning as a function of absolute turning time $t$ [1]. First, the turning delay $\tau_{ij}$ of an agent $i$ with respect to $j$ is calculated by finding the time shift that maximizes the normalized correlation (or overlap) function

$$G_{ij}(\tau) = \frac{\langle \mathbf{u}_i(t) \cdot \mathbf{u}_j(t-\tau)\rangle - \langle \mathbf{u}_i(t)\rangle \cdot \langle \mathbf{u}_j(t-\tau)\rangle}{\sigma_i \sigma_j} \quad \text{(S1)}$$

where $\mathbf{u}_i$ is the radial velocity of agent $i$, $\langle\cdot\rangle$ indicates the time average defined as

$$\langle \mathbf{u}_i(t) \cdot \mathbf{u}_j(t-\tau)\rangle = \int dt \mathbf{u}_i(t) \cdot \mathbf{u}_j(t-\tau), \quad \text{(S2)}$$

and $\sigma_i = \sqrt{(\langle \mathbf{u}_i(t)^2\rangle - \langle \mathbf{u}_i(t)\rangle^2)}$ is the variance and the integral is over the turn duration. A positive value of $\tau_{ij}$ indicates that agent $j$ turned before agent $i$, and vice-versa. Using the mutual delay matrix $\tau_{ij}$, a pairwise comparison matrix

$$w_{ij} = \text{sign}(-\tau_{ij})$$

is constructed, where

$$w_{ij} = \begin{cases} +1 & \text{if agent } i \text{ turns before } j, \\ -1 & \text{if agent } i \text{ turns after } j, \\ 0 & i = j. \end{cases}$$

Then, for each agent $i$, a ranking score $\phi_i = \sum_j w_{ij}$ is computed, summing the number of "wins" over other agents. By sorting agents by decreasing $\phi_i$ , we get a robust turning order (ranks) $r_i$, with rank 1 indicating the first agent to turn. The absolute turning times $t_i$ are then calculated recursively, incorporating the delays relative to all agents that turned earlier, according to

$$t_i = \frac{1}{r_i - 1} \sum_{r_j < r_i} (t_j + \tau_{ij}), \quad r_i > 1,$$

where the top-ranked agent's ($r_{top} = 1$) turning time is set to zero ($t_{top} = 0$). Plotting the rank $r_i$ against the absolute turning time $t_i$ for all agents yields the ranking curve $r(t)$. Given an average density $\varrho$ of the flock, the propagation curve is given by $x(t) = [r(t)/\varrho]^{1/d}$, where $d$ is the system dimension.

## S2. SINGLE AGENT ESCAPE DYNAMICS FROM TWO PREDATORS

To rationalize the simulation results for the escape of flocks from two predators, we consider a simple model for the average flock polarization arising from the interaction with two predators, which considers only a single representative agent:

$$\begin{aligned} \dot{\phi}(x,y) = &\frac{\Omega}{2} \sin(\phi(x,y) - \theta_1(x,y)) \\ &+ \frac{\Omega}{2} \sin(\phi(x,y) - \theta_2(x,y)), \end{aligned} \quad \text{(S3)}$$

with $\dot{x} = \cos\phi$ and $\dot{y} = \sin\phi$. Here, $\theta_1$ and $\theta_2$ are the polar angles of the position vectors between the prey and predator 1 and 2, respectively. If we assume for simplicity that $\theta_1(x,y) = \theta_1$ and $\theta_2(x,y) = \theta_2$, i.e. there is no coupling between position and the measured angle, we obtain the stable fixed point

$$\phi^* = \bar{\theta} + \pi, \quad \text{(S4)}$$

where $\bar{\theta} = (\theta_1 + \theta_2)/2$. This implies that the escape direction point along the perpendicular bisector between the two predators.

A stability analysis of Eq. (S3) then show that a perturbation $\epsilon_0$ decays as

$$\epsilon(t) = \epsilon_0 \exp(-\lambda t), \quad \text{(S5)}$$

toward the fixed point, with

$$\lambda = \tilde{\Omega} = \Omega \cos\left(\frac{\theta_1 - \theta_2}{2}\right). \quad \text{(S6)}$$

Thus, the flock orientation should converges exponentially toward the fixed point $\phi^*$. However, in the simulations we do not observe this behavior, which is due to the positional coupling between $\phi$ and $\theta_{1,2}$.

To see how this instability arises, we include the posi-

* g.gompper@fz-juelich.de

tional dependence in $\dot{\phi}$, as

$$\begin{aligned}\dot{\phi} &= \tilde{\Omega}\sin(\phi-\bar{\theta}),\\ \theta_1 &= \tan^{-1}\left(\frac{L_p\sin\theta - y}{L_p\cos\theta - x}\right),\\ \theta_2 &= \tan^{-1}\left(\frac{-L_p\sin\theta - y}{L_p\cos\theta - x}\right).\end{aligned} \tag{S7}$$

Here, we assume for simplicity $\theta_1 = \theta$ and $\theta_2 = -\theta$ at $t = 0$, so that $\bar{\theta} = 0$. Now consider a perturbation about the fixed point,

$$\phi = \pi + \epsilon, \qquad \text{with } |\epsilon| \ll 1. \tag{S8}$$

Then,

$$\begin{aligned}x(t) &= \cos(\pi+\epsilon)v_0 t \simeq -v_0 t,\\ y(t) &= \sin(\pi+\epsilon)v_0 t \simeq -\epsilon v_0 t.\end{aligned} \tag{S9}$$

We linearize $\dot{\phi} = f(x, y, \phi)$ around $\phi = \pi$, $y = 0$, and fixed $x$,

$$\begin{aligned}\dot{\epsilon} =& f(x,0,\pi) + \left[f'(x,y,\epsilon)\frac{\partial f}{\partial y}\right]_{x,0,\pi}\\ &+ \left[f'(x,y,\epsilon)\frac{\partial f}{\partial \phi}\right]_{x,0,\pi}\end{aligned} \tag{S10}$$

This gives

$$\dot{\epsilon} = -\Omega\frac{D_\parallel}{D}\epsilon - \Omega\frac{D_\parallel^2}{D^3}y \tag{S11}$$

with distances $D = \sqrt{L_p^2 + x^2 - 2L_p x\cos\theta}$ and $D_\parallel = L_p\cos\theta - x$. The second derivative then becomes

$$\ddot{\epsilon} + \Omega\frac{D_\parallel}{D}\dot{\epsilon} - \Omega\frac{v_0 D_\parallel^2}{D^3}\epsilon = 0. \tag{S12}$$

Thus, we obtain an oscillator equation with an inverted harmonic potential, i.e. an unstable damped oscillator. Thus, when positional coupling is included, the fixed point $\phi^* = \pi$ becomes unstable, and perturbations $\epsilon$ grow with time. However, since the perturbation term decays as $1/D$, $\epsilon$ saturates to a constant with increasing distance from the predators, i.e. for long times. This also implies that the displacement component perpendicular to the bisector initially increases before it asymptotically saturates. The spread is larger due to stronger growth of the perturbation for shorter distances $D$ (i.e. $L_p$), compare Fig. S5(a,b) and Fig. S5(c,d).

Consequently, an ensemble of particles initially located at different $y$ positions evolves in different directions, rather than converging to the fixed point that is stable in the absence of positional coupling. The simulations data showing the spread in the exit angles Fig. S4(a) and some sample trajectories Fig. S4(b,c) confirm the result of this calculation. Importantly this implies that for a flock, different border agents *pull* the flock in different directions – in addition to the blocked vision of these agents on one or the other predator. The flocks final trajectory depends on which border *wins*. Figure S2, S3 shows the data for single particles and for flock for all investigated $\Delta\Theta$.

## S3. FLOCK SHAPE

### 1. Gyration tensor and asphericity

We approximate the shape of a particle ensemble using the gyration tensor computed from its 2D positions. Given particle coordinates $\{\mathbf{r}_i\}_{i=1}^N$, we first define:

$$\mathbf{r}_i' = \mathbf{r}_i - \langle\mathbf{r}\rangle \tag{S13}$$

We then compute the gyration tensor:

$$\mathbf{G} = \frac{1}{N}\sum_{i=1}^{N}\mathbf{r}_i'\mathbf{r}_i'^T \tag{S14}$$

Diagonalization of $\mathbf{G}$ yields the eigenvalues $\lambda_1 \geq \lambda_2$ and corresponding eigenvectors $\mathbf{u}$, $\mathbf{v}$. The asphericity is then defined as:

$$A = \frac{\lambda_1 - \lambda_2}{\lambda_1 + \lambda_2} \tag{S15}$$

### 2. Ellipsoidal approximation and visibility model

We approximate the structure as an ellipse centered at the mean position $\langle\mathbf{r}\rangle$. The semi-axis lengths are derived from the eigenvalues to be: $a = 2\sqrt{\lambda_1}$, $\quad b = 2\sqrt{\lambda_2}$ and the corresponding orthonormal directions are given by eigenvectors $\mathbf{u}$ and $\mathbf{v}$. A boundary point on the ellipse is parameterized as:

$$\mathbf{x}(t) = \mathbf{c} + a\cos s\,\mathbf{u} + b\sin s\,\mathbf{v}, \quad s \in [0, 2\pi] \tag{S16}$$

Given a threat position $\mathbf{p}$, we define that a boundary point $\mathbf{x}(s)$ can *detect* the threat if its outward normal points toward the threat:

$$\mathbf{n}(s)\cdot(\mathbf{p} - \mathbf{x}(s)) > 0 \tag{S17}$$

where the outward normal in the ellipse frame is approximated by:

$$\mathbf{n}(s) = \left(\frac{\cos s}{a}, \frac{\sin s}{b}\right) \tag{S18}$$

We discretize the boundary into $N_b$ uniformly spaced angles $s_i$. The reacting fraction of agents for a threat $\mathbf{p}$ is estimated as:

$$f_p = \frac{1}{N_b}\sum_{i=1}^{N_b}\mathbb{I}\left[\mathbf{n}(t_i)\cdot(\mathbf{p} - \mathbf{x}(s_i)) > 0\right] \tag{S19}$$

For two threats $\mathbf{p}_1$ and $\mathbf{p}_2$, we define the joint visibility fraction as

$$\begin{aligned}f_{\text{both}} = \frac{1}{N_b}\sum_{i=1}^{N_b}\mathbb{I}[&\mathbf{n}(s_i)\cdot(\mathbf{p}_1 - \mathbf{x}(s_i)) > 0\\ &\wedge\, \mathbf{n}(s_i)\cdot(\mathbf{p}_2 - \mathbf{x}(s_i)) > 0]\end{aligned} \tag{S20}$$

Figure S6 shows an example implementation.

## S4. MOVIE CAPTIONS

**Movie M1:** Propagating information wave (blue) in a flock for $\eta = 0.1$ and $\eta = 1.0$, with fixed $v_0 = 0.2$, $\Delta_p = 0.05$. Threat position shown in red.

**Movie M2:** Flock splitting due to penetration of the flock by a motile threat for $v_p/v_0 = 1.25$ and $v_p/v_0 = 2.25$, $\eta = 2.0$, and flock velocity $v_0 = 0.2$.

**Movie M3:** Flock scattering in response to two fixed threat for $\Delta\Theta = 4\Delta\theta$ for two different simulations runs with identical parameter values ($v_0 = 0.2$, $\eta = 2.0$, $\Delta_p = 0.06$). Here the threat positions are not to scale and are shown closer for better visualization. Threats are at distance $L_p = 200$ from flock center.

[1] A. Attanasi, A. Cavagna, L. Del Castello, I. Giardina, T. S. Grigera, A. Jelić, S. Melillo, L. Parisi, O. Pohl, E. Shen, et al., Nature Physics **10**, 691 (2014), ISSN 1745-2481, URL https://www.nature.com/articles/nphys3035.

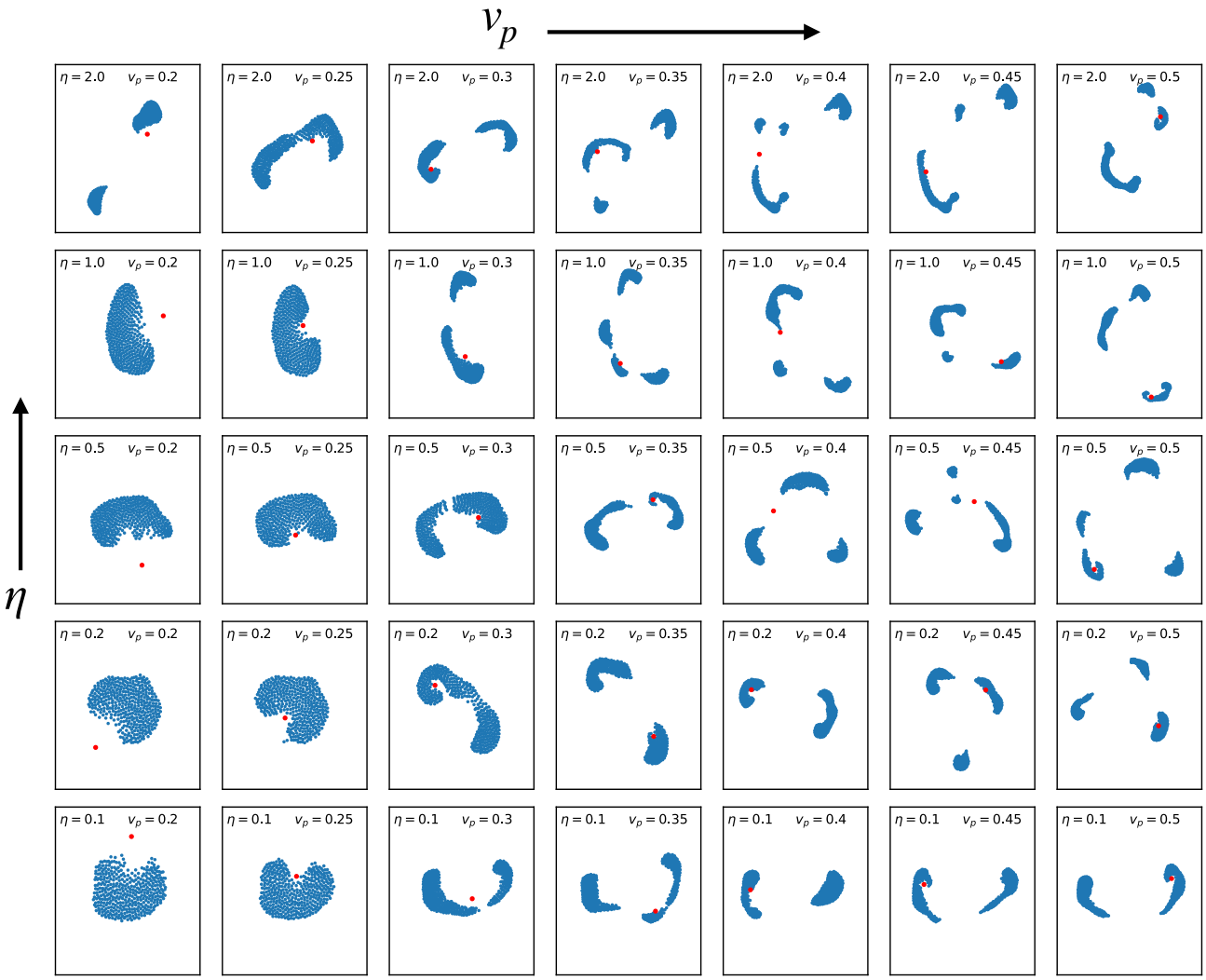



FIG. S1. **Flock-splitting snapshots.** Snapshots of the flock at time $t = 2t_L$ ($t_L = \sqrt{N}R_a/v_0$ is characteristic time required to traverse the flock size) for different predator speeds $v_p$ (columns) and $\eta$ values (rows). As $v_p$ increases, the flock splits into several smaller clusters. The flock speed is fixed at $v_0 = 0.2$

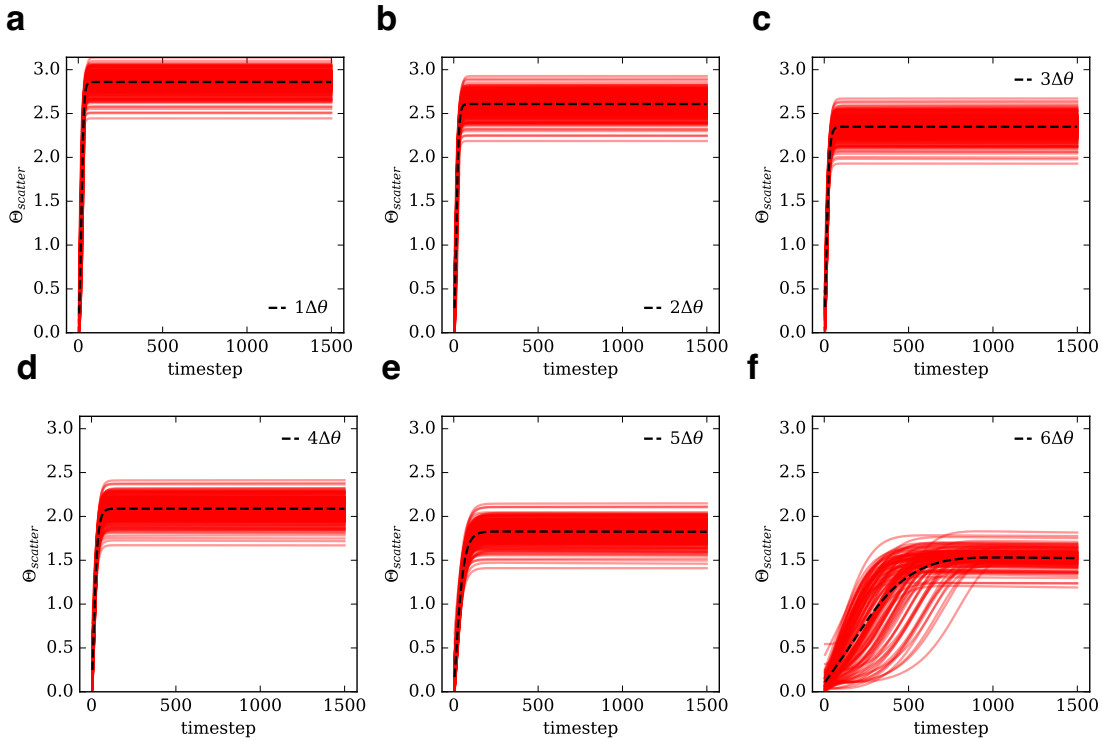



FIG. S2. (a-f) Angle of particle polarization for *non-interacting particles*, for 400 different particles simulations at different predator angular separation $\Delta\Theta$. (g-l) Angle of the average *flock* polarization for 100 different particles and different predator angular separation $\Delta\Theta$.

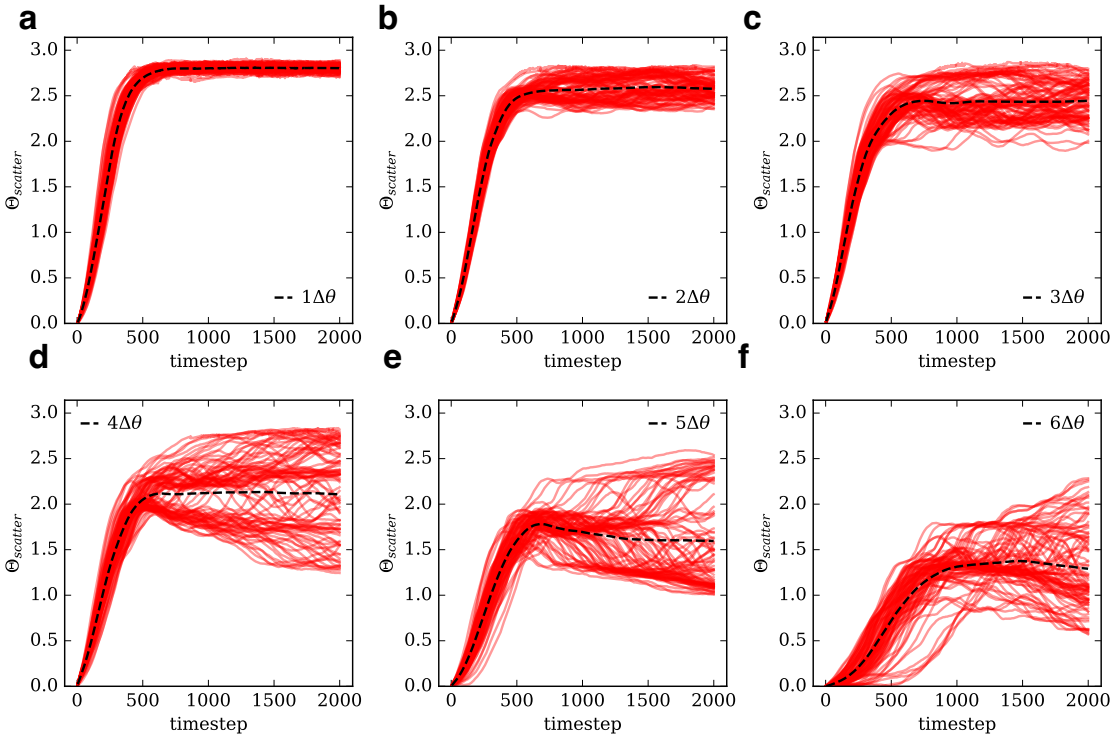



FIG. S3. (a-f) Angle of the average *flock* polarization for 100 different particles and different predator angular separation $\Delta\Theta$.

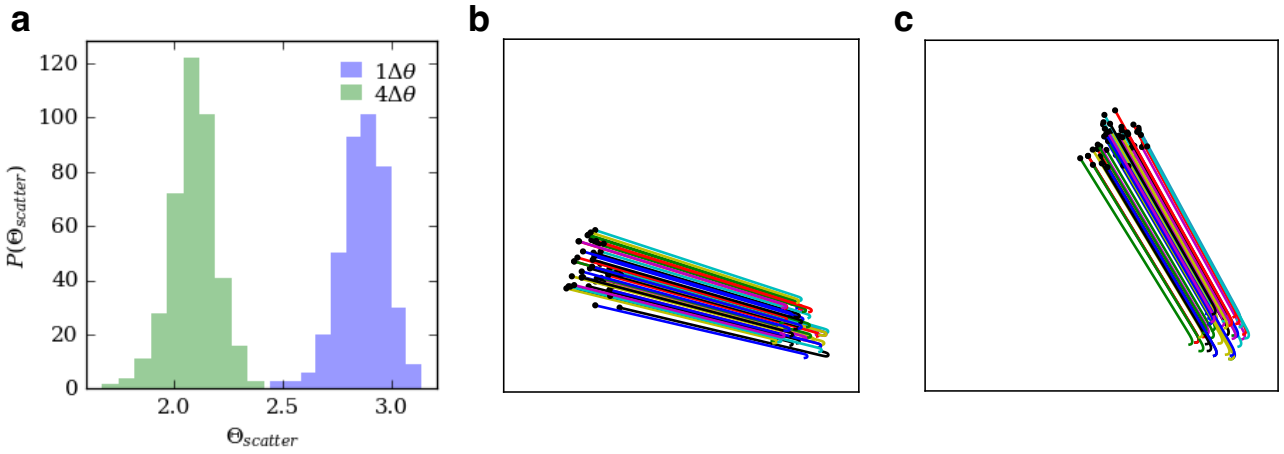



FIG. S4. (a) Probability distribution of the scattering angle for individual particles reacting to threats with $\Delta\Theta = 1\Delta\theta$ and$\Delta\Theta = 4\Delta\theta$, and (b,c) corresponding trajectories. Data are shown for 400 independent simulations.

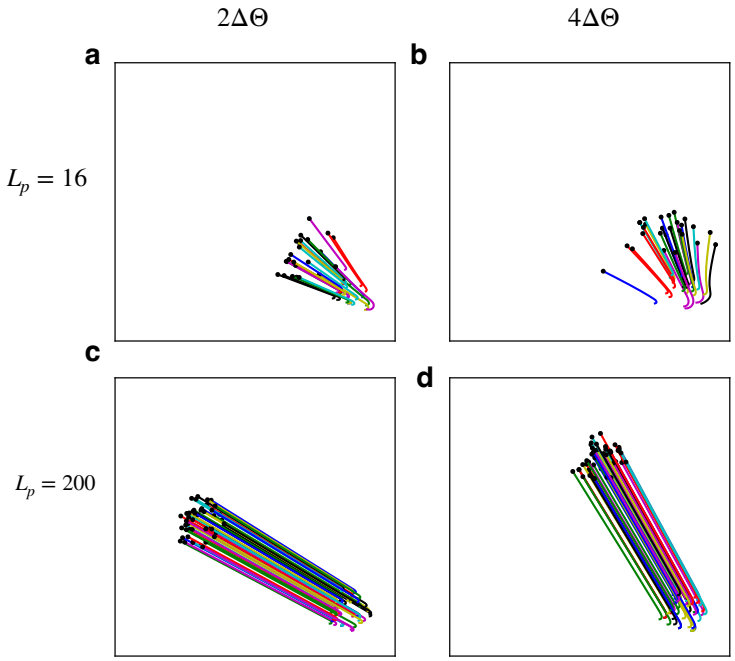



FIG. S5. Single particle trajectories for various initial predator distances $L_p$ and angular separations $\Delta\Theta$.

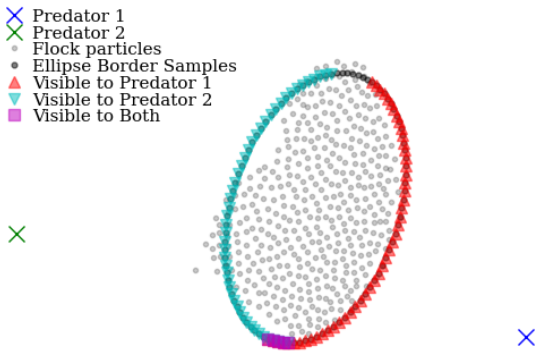



FIG. S6. **Flock shape and local predator perception.** Snapshot of a typical conformation of a flock, where particles of the flock (grey circles) form a compact group, with a boundary (black dots) well approximated by an ellipse. Colored segments of the boundary indicate portions from which one or both predators are visible. The predator positions are schematic and are not drawn to scale; they are shown only to illustrate the corresponding visible border fractions. Here $\Delta\Theta = 5\Delta\theta$.